RSC Advances

PAPER

View Article Online
View Journal | View Issue

Cite this: *RSC Adv.*, 2020, **10**, 4772

Effect of fatty acids on the accelerated sulfur vulcanization of rubber by active zinc/carboxylate complexes†

Preeyanuch Junkong,[ab] Rie Morimoto,[c] Kosuke Miyaji,[ac] Atitaya Tohsan,[ad] Yuta Sakaki[ac] and Yuko Ikeda *[ae]

Received 10th December 2019
Accepted 18th January 2020

DOI: 10.1039/c9ra10358a

rsc.li/rsc-advances

The effect of fatty acids with different aliphatic chain lengths on the accelerated vulcanization reaction of isoprene rubber was investigated through the generation of new intermediates composed of dinuclear bridging bidentate zinc/carboxylate complexes. Using the combination of *in situ* time-resolved Fourier-transform infrared spectroscopy and *in situ* time-resolved zinc K-edge X-ray absorption fine structure spectroscopy, the essential complex structure of the intermediates formed during the vulcanization reaction of isoprene rubber was determined to be independent of the aliphatic chain length of fatty acids. However, the reactivity of arachidic acid with ZnO was found to be low, which prolonged the induction period and curing time, and slowed down the curing rate in the vulcanization of isoprene rubber. These results help to understand the complicated vulcanization reaction of rubber, especially natural rubber, which inherently contains various fatty acids. The results obtained in this study are important for developing well-designed high-performance natural rubber products in the future.

Introduction

Almost all useful rubber products have to be a three-dimensionally cross-linked network for displaying stable elasticity. Among various cross-linking reactions, the most widely used in the rubber industry is vulcanization, *i.e.*, cross-linking with sulfur. Vulcanization was first developed by Goodyear in 1839. Since then, additives such as accelerators, activators, and retarders have been developed for the improvement in processability and mechanical properties of rubber products.[1–10] Activators have been described as substances that increase the effects of accelerators. Activators are divided into two categories: organic and inorganic. Fatty acids and their derivatives are typical organic activators, and metal-based compounds such as zinc oxide (ZnO) are often used as an inorganic activator in vulcanization.[1,5,6] By far, the most popular vulcanization activator system is composed of ZnO and stearic acid (StH). ZnO reacts with the StH to form zinc stearate, which is soluble in the rubber and facilitates the cross-linking reaction.

In 2009, using the advantageous small-angle neutron scattering, our group found that a combining ZnO with the other cross-linking reagents was crucial not only for chemical cross-linking but also for controlling structural network inhomogeneity in the sulfur cross-linked isoprene rubber.[11] The two-phase inhomogeneous network structure of the sulfur cross-linked isoprene rubber consisting of the domains of high network-chain density which were embedded in the rubber network matrix (the mesh network) was proposed. Interestingly, the mesh size in the two-phase inhomogeneous structure was revealed to be controlled by the amounts of ZnO and StH. Surprisingly, *in situ* time-resolved zinc K-edge X-ray absorption fine structure (XAFS) spectroscopy indicated that two different sulfur cross-linking reactions for the two-phase network formation were found to occur mostly together.[12] However, the form of the zinc salt of StH has not been well understood.[1–9] The role of the zinc salt of StH during the vulcanization reaction has not been exhaustively studied. In our previous work, on the other hand, a combination of *in situ* time-resolved zinc K-edge XAFS spectroscopy, *in situ* time-resolved Fourier-transform infrared (FT-IR) spectroscopy, and density functional theory (DFT) calculations was used to determine the role of the zinc salt of StH. It was worth noting that a new complex generated from ZnO and StH at high temperature was formed.[13]

A dominant structure was bridging bidentate zinc/stearate complex, where the zinc cation:stearate molar ratio of the

[a]*Center for Rubber Science and Technology, Kyoto Institute of Technology, Matsugasaki, Sakyo, Kyoto 606-8585, Japan. E-mail: yuko@kit.ac.jp*
[b]*Faculty of Science, Mahidol University, Ratchathewi, Bangkok 10400, Thailand*
[c]*Graduate School of Science and Technology, Kyoto Institute of Technology, Matsugasaki, Sakyo, Kyoto 606-8585, Japan*
[d]*Faculty of Engineering, King Mongkut's University of Technology North Bangkok, 1518 Pracharat 1 Rd, Wongsawang, Bangsue, Bangkok 10800, Thailand*
[e]*Faculty of Molecular Chemistry and Engineering, Kyoto Institute of Technology, Matsugasaki, Sakyo, Kyoto 606-8585, Japan*

† Electronic supplementary information (ESI) available: FT-IR spectra of (a) IR-ZnO(0.5)-LaH(1.4), (b) IR-ZnO(0.5)-MyH(1.6), (c) IR-ZnO(0.5)-PaH(1.8), (d) IR-ZnO(0.5)-StH(2.0) (e) IR-ZnO(0.5)-ArH(2.2) and (f) IR-$ZnSt_2$(4.5) at 144 °C in the ranges of 4000–400 cm^{-1}, and 1820–1350 cm^{-1}. See DOI: 10.1039/c9ra10358a

complex was surprisingly 2 : 2. The DFT calculation suggested the fundamental skeleton of dinuclear type bridging bidentate zinc/stearate complex to be composed of $[Zn_2(\mu\text{-}O_2CC_{17}H_{35})_2]^{2+}\cdot 4X$, where X is hydroxyl group, water and/or rubber segment (the intermediate **I**) as shown in Fig. 1. Particularly, the calculation showed the existence of two hydroxyl groups with water and/or a rubber segment in the complex.[13] This intermediate has been unknown despite the long history of rubber science and technology. The newly observed zinc/stearate complex acts as an enzyme to accelerate the sulfur cross-linking reaction of rubber.

In 2019, we finally revealed the vulcanization mechanism *via* the intermediate **I**,[14] where the hydrolysis reaction of *N*-cyclohexyl benzothiazole sulfenamide (CBS), the insertion reaction of sulfur and sulfur cross-linking reaction were found to be accelerated. Furthermore, the visualization of this speculated two-phase morphology was confirmed by using the atomic force microscopy nanomechanical mapping with the two-dimensional mapping of reliability index.[15] Without StH, the average Young's modulus of mesh network in the matrix of the sulfur cross-linked isoprene rubber was found to be very low, possibly attributed to the lack of intermediate of zinc/stearate complex inducing the mesh network formation. Furthermore, using a linear combination fitting in sulfur K-edge X-ray absorption near edge structure measurements for the solvent extracted sulfur cross-linked isoprene rubber, the sulfidic linkage of a disulfidic type was found to be dominant in the CBS-accelerated system when either zinc stearate[16] or a combination of ZnO and StH[17] were used as the activators. Importantly, the presence of the bridging bidentate zinc/stearate complex as an intermediate for the sulfur cross-linking reaction was suggested to induce the generation of abundant disulfidic linkages in the rubber networks.

However, the role of organic activators, fatty acids, has still received much less research effort than other components in the rubber compound, although natural rubber contains several kinds of fatty acids.[10] The effectiveness of fatty acids in activation of vulcanization is a function of its solubility in rubber, which relates to the molecular weight and melting point. Normally, the fatty acids employed for the vulcanization have 12–18 carbon atoms in rubber industry. In order to prevent the side reaction of vulcanization, in this work, the influence of different saturated fatty acid types, *i.e.*, various aliphatic chain lengths, on the reactivity to ZnO during mixing and on the generation of intermediate in dinuclear type bridging bidentate zinc/carboxylate complex are investigated by *in situ* measurements of zinc K-edge XAFS spectroscopy and *in situ* time-resolved FT-IR spectroscopy. Characteristics of vulcanization reactions by various kinds of fatty acid are reported for the first time in this study.

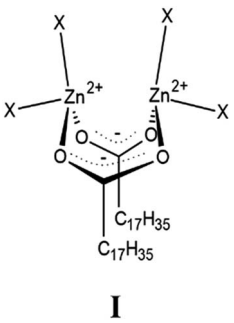

I

Fig. 1 Dinuclear type bridging bidentate zinc/stearate complex (labelled as the intermediate **I**), where X is hydroxyl group, water and/or rubber segment. Reprinted with permissions from ref. 13 and 14, Copyright 2015 and 2019 American Chemical Society.

Experimental

Materials

Isoprene rubber (IR2200) was supplied from JSR Co, Japan. Natural rubber (NR, RSS no. 1) was used. Elemental sulfur (S_8, purity: 99.9%, powder: 150 mesh), ZnO (average diameter: 0.29 μm), *N*-cyclohexyl-2-benzothiazole sulfenamide (CBS, Sanceler CM-G), and zinc stearate ($ZnSt_2$) were rubber-processing commercial grade and used as received. They were purchased from Hosoi Chemical Industry Co., Ltd., Tokyo, Japan, Sakai Chemical Industry Co., Ltd., Osaka, Japan, Sanshin Chemical Industry Co., Ltd., Yamaguchi, Japan, and FUJIFILM Wako Pure Chemical Corporation., Osaka, Japan, respectively. Different kinds of saturated fatty acid, *i.e.*, lauric acid (LaH, C_{12}, purity: >98.0%), myristic acid (MyH, C_{14}, purity: >99.0%), palmitic acid (PaH, C_{16}, purity: >99.5%), and arachidic acid (ArH, C_{20}, purity: >98.0%) were purchased from Tokyo Chemical Industry Co., Tokyo, Japan. Stearic acid (StH, C_{18}, LUNAC S-25) was supplied from Kao Co., Tokyo, Japan. All fatty acids were used as received.

Sample preparation

The rubber compounds were prepared according to the recipes shown in Table 1 by conventional mixing at room temperature for about 20 min on a two-roll mill with a water-cooling system (6 × 15 test roll, Kansai Roll Co., Ltd., Osaka, Japan). Amounts of the reagents are shown in units of "mol g^{-1}" and "parts per one hundred rubbers by weight (phr)". The latter is a conventional unit in rubber science and technology. Abbreviations for all samples were assigned based on the combinations of reagents, *e.g.*, ZnO, S_8, CBS, $ZnSt_2$, LaH, MyH, PaH, ArH, and StH. The "IR", "NR" and the numbers in parentheses in the sample codes indicate isoprene rubber, natural rubber and the amount of each reagent mixed with each rubber in phr, respectively. The rubber compounds prepared in this study were divided into two systems, which are the unvulcanised system (mixed with ZnO and fatty acid only) and the vulcanization system. Here, IR mixed with $ZnSt_2$ (IR-$ZnSt_2$(4.5)) or ZnO (IR-ZnO(1)) are reference samples.

Fourier-transform infrared spectroscopy

In situ time-resolved Fourier-transform infrared spectroscopy (FT-IR) was performed at 32 scans for 40 s every 44 s across the wavenumber range 4000–400 cm^{-1} by a single-reflection attenuated total reflectance (ATR) method on a diamond plate

Table 1 Sample recipes used in this study in phr[a] and mol g^{-1} of rubber

Sample code	Unit	IR[b]	ZnO[c]	LaH[d]	MyH[e]	PaH[f]	StH[g]	ArH[h]	$ZnSt_2$[i]	CBS[j]	S_8[k]
IR-ZnO(0.5)-LaH(1.4)	phr	100	0.50	1.41	—	—	—	—	—	—	—
	mol g^{-1}		6.14×10^{-3}	7.03×10^{-3}	—	—	—	—	—	—	—
IR-ZnO(0.5)-LaH(1.4)-CBS(1)-S_8(1.5)	phr	100	0.50	1.41	—	—	—	—	—	1.00	1.50
	mol g^{-1}		6.14×10^{-3}	7.03×10^{-3}	—	—	—	—	—	3.78×10^{-3}	5.85×10^{-3}
IR-ZnO(0.5)-MyH(1.6)	phr	100	0.50	—	1.61	—	—	—	—	—	—
	mol g^{-1}		6.14×10^{-3}	—	7.03×10^{-3}	—	—	—	—	—	—
IR-ZnO(0.5)-MyH(1.6)-CBS(1)-S_8(1.5)	phr	100	0.50	—	1.61	—	—	—	—	1.00	1.50
	mol g^{-1}		6.14×10^{-3}	—	7.03×10^{-3}	—	—	—	—	3.78×10^{-3}	5.85×10^{-3}
IR-ZnO(0.5)-PaH(1.8)	phr	100	0.50	—	—	1.80	—	—	—	—	—
	mol g^{-1}		6.14×10^{-3}	—	—	7.03×10^{-3}	—	—	—	—	—
IR-ZnO(0.5)-PaH(1.8)-CBS(1)-S_8(1.5)	phr	100	0.50	—	—	1.80	—	—	—	1.00	1.50
	mol g^{-1}		6.14×10^{-3}	—	—	7.03×10^{-3}	—	—	—	3.78×10^{-3}	5.85×10^{-3}
IR-ZnO(0.5)-StH(2.0)	phr	100	0.50	—	—	—	2.00	—	—	—	—
	mol g^{-1}		6.14×10^{-3}	—	—	—	7.03×10^{-3}	—	—	—	—
IR-ZnO(0.5)-StH(2.0)-CBS(1)-S_8(1.5)	phr	100	0.50	—	—	—	2.00	—	—	1.00	1.50
	mol g^{-1}		6.14×10^{-3}	—	—	—	7.03×10^{-3}	—	—	3.78×10^{-3}	5.85×10^{-3}
IR-ZnO(0.5)-ArH(2.2)	phr	100	0.50	—	—	—	—	2.20	—	—	—
	mol g^{-1}		6.14×10^{-3}	—	—	—	—	7.03×10^{-3}	—	—	—
IR-ZnO(0.5)-ArH(2.2)-CBS(1)-S_8(1.5)	phr	100	0.50	—	—	—	—	2.20	—	1.00	1.50
	mol g^{-1}		6.14×10^{-3}	—	—	—	—	7.03×10^{-3}	—	3.78×10^{-3}	5.85×10^{-3}
IR-$ZnSt_2$(4.5)	phr	100	—	—	—	—	—	—	4.50	—	—
	mol g^{-1}		—	—	—	—	—	—	6.80×10^{-5}	—	—
IR-ZnO(1)	phr	100	1.0	—	—	—	—	—	—	—	—
	mol g^{-1}		12.2×10^{-5}	—	—	—	—	—	—	—	—
NR-ZnO(0.5)	phr	100	0.50	—	—	—	—	—	—	—	—
	mol g^{-1}		6.14×10^{-3}	—	—	—	—	—	—	—	—

[a] Parts per one hundred rubbers by weight. [b] Isoprene rubber. [c] Zinc oxide. [d] Lauric acid. [e] Myristic acid. [f] Palmitic acid. [g] Stearic acid. [h] Arachidic acid. [i] Zinc stearate. [j] *N*-Cyclohexyl-2-benzothiazolesulfenamide. [k] Sulfur.

(GradiATR, PIKE Technologies, Wisconsin, USA) in an IR Prestige-21 instrument (Shimadzu Co., Kyoto, Japan). The resolution was 4 cm^{-1}. The temperature was kept at 35 °C for 5 min, was increased from 35 to 144 °C for 10 min at approximately 16 °C min^{-1}, and was maintained at 144 °C for a specific time according to a controlled program. The temperature was controlled to less than ±1 °C. The sample area was about 2 × 3 mm^2 and the thickness was approximately a few millimetres. The peak assignments for the FT-IR spectra of IR-ZnO(0.5)-LaH(1.4), IR-ZnO(0.5)-MyH(1.6), IR-ZnO(0.5)-PaH(1.8), IR-ZnO(0.5)-StH(2.0) and IR-ZnO(0.5)-ArH(2.2) in Fig. S1† are described in Table S1.† Differential FT-IR spectra were obtained by subtracting the spectrum of isoprene rubber from each original spectrum; the base line was from 1820 to 700 cm^{-1}.

Rheometer measurement

Curing behavior of rubber compounds was measured using MR-500 (UBM Co., Kyoto, Japan) at 1 Hz of frequency and rotation angle between 0.01° and 15°. The temperature was kept at 35 °C for 5 min, was increased from 35 to 144 °C for 10 min at approximately 16 °C min^{-1}, and was maintained at 144 °C for a specific time according to a controlled program. Shear storage modulus (G') and shear loss modulus (G'') as well as the cure curves were investigated. Because the torque change in rheology

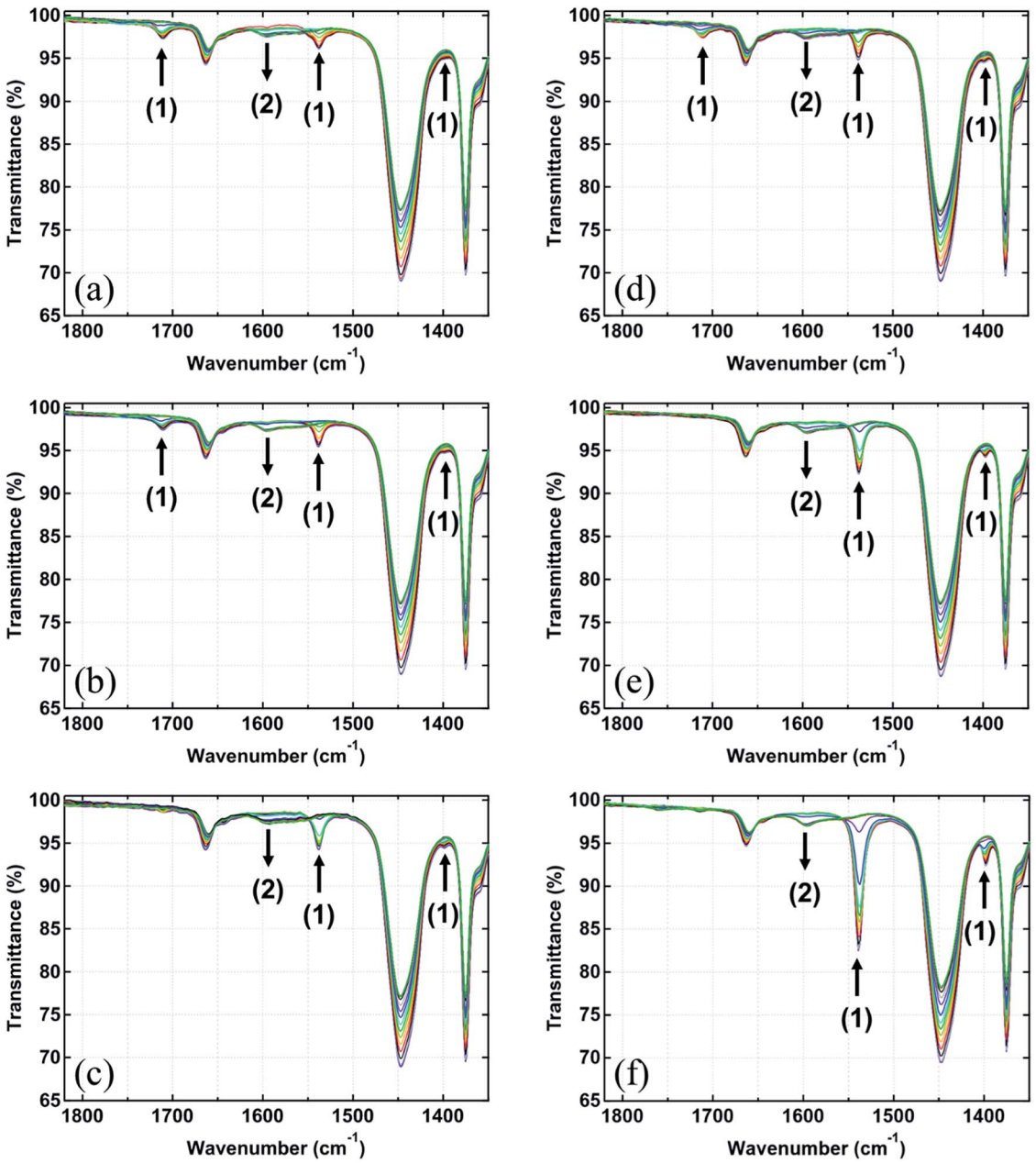

Fig. 2 FT-IR spectra of the heating process from 35 to 144 °C and the constant temperature condition at 144 °C for (a) IR-ZnO(0.5)-LaH(1.4), (b) IR-ZnO(0.5)-MyH(1.6), (c) IR-ZnO(0.5)-PaH(1.8), (d) IR-ZnO(0.5)-StH(2.0), (e) IR-ZnO(0.5)-ArH(2.2) and (f) IR-$ZnSt_2$(4.5) in the range of 1820–1350 cm^{-1}. Numbers and black arrows indicate the order and the direction of band shifts during heating, respectively.

measurement is proportional to the network-chain density, the rate equation of vulcanization can be expressed in the velocity (V) of the torque change as the following equation:[18]

$$V = -\mathrm{d}(M_\mathrm{H} - M_t)/\mathrm{d}t = K(M_\mathrm{H} - M_t)^n \quad (1)$$

where, M_H is the maximum torque, M_t is the torque at vulcanization time t, K is a rate constant and n is the order of the reaction. In the curing period, the rate of reaction is known to follow the first order reaction.[18] For the first-order reaction of eqn (1) can be written as:

$$\ln(M_\mathrm{H} - M_t) = \ln B - K(t - t_0) \quad (2)$$

where, B is a constant and t_0 is induction time. Therefore, the parameter K can be determined from the slope of the plot between $\ln(M_\mathrm{H} - M_t)$ and $(t - t_0)$.

Differential scanning calorimetry

Differential scanning calorimetry (DSC) measurements were carried out using Rigaku Thermoflex (DSC-82300, Rigaku Co., Tokyo, Japan) under nitrogen atmosphere. The temperature was kept at 35 °C for 5 min, was increased from 35 to 144 °C for 10 min at approximately 16 °C min^{-1}, and was maintained at 144 °C for a specific time according to a controlled program. The amount of the sample mass was approximately 10 mg encapsulated in an aluminium pan.

Zinc K-edge X-ray absorption fine structure spectroscopy

In situ synchrotron zinc K-edge X-ray absorption fine structure (XAFS) measurements were carried out every 78 s at BL-14B2 beamline of SPring-8 in Harima, Japan.[19] The rubber compound was sealed in a Teflon® tube with Kapton® windows and then heated in a laboratory-made reaction cell according to a controlled program, which was set to heat at 35 °C for approximately 8 min, from 35 to 144 °C for 10 min at approximately 16 °C min^{-1}, and to hold the temperature at 144 °C for a specific time. The temperature control error was less than ±1 °C. The sample was cylindrical; the diameter was 10 mm and the length was based on the molar concentration of each element in the sample, determined using XAFS_SAMPLE software.[20] An irradiation time of X-ray was 52 s. Si(311) crystal was used as the monochromators. The X-ray absorption spectra for the samples were recorded in a transmission mode using ionization chambers. The XAFS spectra were analyzed with the ATHENA and ARTEMIS XAFS analysis package[21] and FEFF6.02L.[22,23] For quantitative analyses of XAFS spectra, a linear combination fitting method was conducted in an energy range from 9619 to 9739 eV using a routine linear combo method in ATHENA. Then, the concentration of zinc atom of all the samples fitted by each reference model can be determined as eqn (3).

$$N_x\ (\mathrm{mol\ g^{-1}}) = N \times W_x \quad (3)$$

where N_x is the concentration of zinc atom (mol g^{-1}), N is the total amount of zinc atom in each sample, W_x is the weight fraction of each reference component in the sample obtained by fitting.

Results and discussion

Generation of dinuclear bridging bidentate zinc/carboxylate complexes from various fatty acids

FT-IR analysis. Fig. 2 and S2† show the *in situ* FT-IR spectra of all isoprene rubber compounds in the unvulcanized systems, *i.e.*, IR-ZnO(0.5)-LaH(1.4), IR-ZnO(0.5)-MyH(1.6), IR-ZnO(0.5)-PaH(1.8), IR-ZnO(0.5)-StH(2.0), IR-ZnO(0.5)-ArH(2.2) and IR-$ZnSt_2$(4.5) from 35 °C to 144 °C in the range of 1820–1350 cm^{-1}. In addition to the characteristic absorption bands of isoprene rubber [*e.g.*, 1663 cm^{-1} (C=C stretching), 1447 cm^{-1} (C–H bending), and 1375 cm^{-1} (C–H symmetrical bending)], the band at 1540 cm^{-1} (COO^- antisymmetric tetrahedral stretching) was

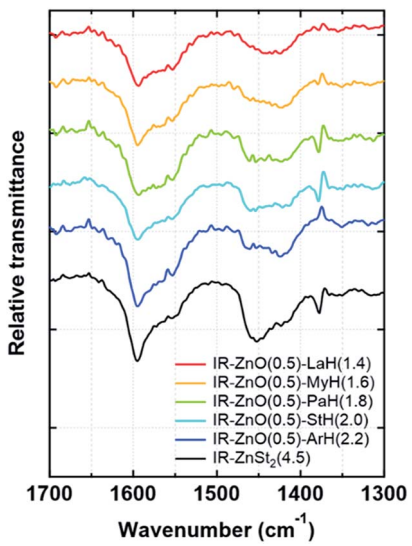

Fig. 3 Differential FT-IR spectra of the samples subtracted using a spectrum of raw isoprene rubber at 144 °C in the range of 1700–1300 cm^{-1}.

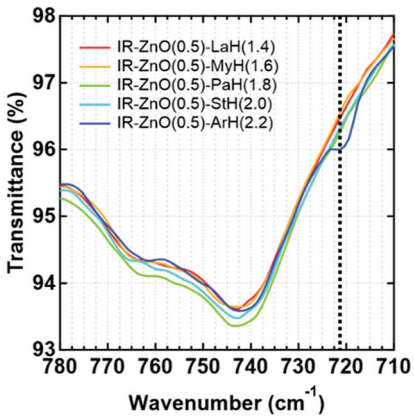

Fig. 4 FT-IR spectra of IR-ZnO(0.5)-LaH(1.4), IR-ZnO(0.5)-MyH(1.6), IR-ZnO(0.5)-PaH(1.8), IR-ZnO(0.5)-StH(2.0) and IR-ZnO(0.5)-ArH(2.2) at 144 °C in the range of 780–710 cm^{-1}.

detected in the spectra of all samples at 35 °C. Note that the band at 1398 cm^{-1} (COO^- symmetric stretching) in the spectra was small, but it was clearly seen after the subtraction by a spectrum of raw isoprene rubber (Fig. S2†). In the common rubber compounding containing StH and ZnO, it is well-known that StH reacts with ZnO to form $ZnSt_2$ as an essential cure activator for the vulcanization reaction. In our previous study, the generation of $ZnSt_2$ was confirmed by the presence of COO^- antisymmetric and symmetric stretching bands at 1537 and 1398 cm^{-1}, respectively, for the spectra of IR-ZnO(0.5)-StH(2) at

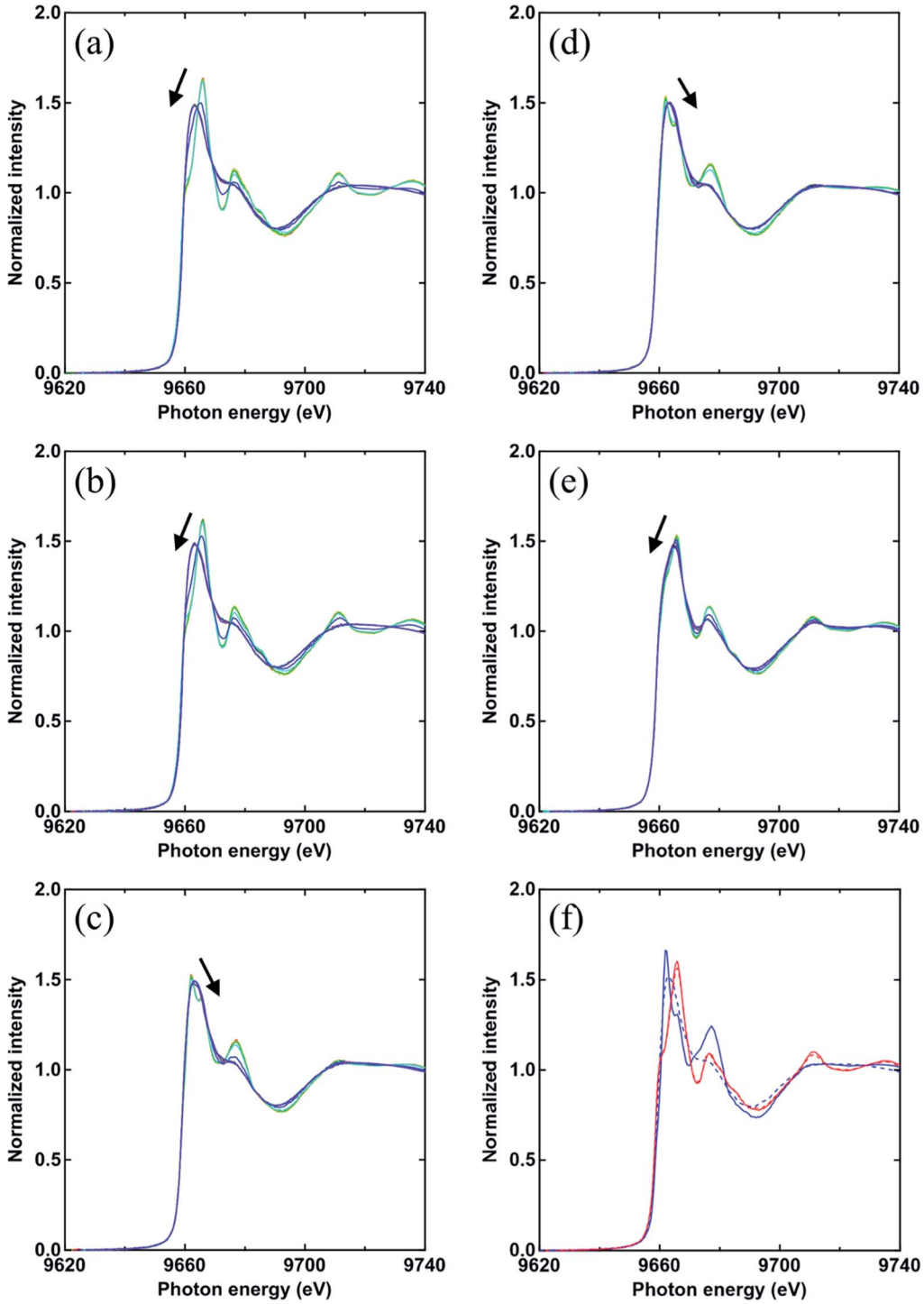

Fig. 5 Variation of zinc K-edge XAFS spectra of the heating process from 35 to 144 °C and the constant temperature condition at 144 °C for (a) IR-ZnO(0.5)-LaH(1.4), (b) IR-ZnO(0.5)-MyH(1.6), (c) IR-ZnO(0.5)-PaH(1.8), (d) IR-ZnO(0.5)-StH(2.0), and (e) IR-ZnO(0.5)-ArH(2.2) in the range of 9620–9740 eV. Black arrows indicate the change of spectra with increasing heating temperature and time. (f) Zinc K-edge XAFS spectra of the reference samples; IR-ZnO and IR-$ZnSt_2$ at 35 °C (solid lines) and 144 °C (dotted lines) in the range of 9620–9740 eV.

35 °C.[13,14] This observation corresponds well with the bands detected in IR-ZnO(0.5)-StH(2.0) and IR-$ZnSt_2$(4.5) at 35 °C in this study. Thus, the bands of COO^- antisymmetric and symmetric stretching that are present in other samples suggest that the reaction between ZnO and each fatty acid also partially occurred during the rubber mixing process.

Upon heating to 144 °C, the absorption band at 1398 cm^{-1} disappeared, and the singlet at 1540 cm^{-1} split into one broad band at 1595 cm^{-1} and one shoulder band at approximately 1560 cm^{-1} in all samples as shown in Fig. 2 and S2.† These changes in their FT-IR spectra were similar to those of ZnO(0.5)-StH(2) and IR-$ZnSt_2$(4.5) in our previous papers,[13,14] where the formation of a specific structural complex was reported. The identified structure was $[Zn_2(\mu\text{-}O_2CC_{17}H_{35})_2]^{2+}\cdot 4X$, where X was a hydroxyl group, water and/or rubber segment (intermediate **I**), as shown in Fig. 1. Therefore, the FT-IR spectra of all samples in this study clearly suggest the generation of bridging bidentate zinc/carboxylate complexes like intermediate **I** in the isoprene rubber matrix at high temperature. The generation did not depend on the aliphatic chain length of the fatty acids. These newly observed intermediates may also accelerate the sulfur cross-linking reaction of rubber.

The COO^- binding modes of all samples were assigned based on the values of separation between the COO^- antisymmetric and symmetric stretching bands [$\Delta\nu$ $cm^{-1} = \nu_{as}(COO^-) - \nu_s(COO^-)$] in their FT-IR spectra. Generally, the value of $\Delta\nu$ below 120 cm^{-1} frequently indicates a chelating carboxylate group, whereas the ionic COO^- group or *syn–syn* bridging coordination and the monodentate coordination show the value of $\Delta\nu = 170 \pm 10$ cm^{-1} and above 180 cm^{-1}, respectively.[24,25] Therefore, this information was used to confirm the structure of the dinuclear bridging bidentate zinc/carboxylate complex at 144 °C in each sample.

In Fig. 3, the FT-IR spectra of all samples at 144 °C (24.4 min after heating) subtracted by that of raw isoprene rubber in the range of 1700–1300 cm^{-1} are shown. In the FT-IR spectra, it is observed that all samples show the same positions of COO^- antisymmetric and symmetric stretching of the zinc/carboxylate complexes that are weakly coordinated with water at 1595 and 1422 cm^{-1}, respectively. These results agree well with the absorption bands observed in IR-ZnO(0.5)-StH(2) at 144 °C in our previous study.[13,14] In addition, $\Delta\nu$ of the COO^- antisymmetric and symmetric stretching of these two bands was 173 cm^{-1} for all samples. Therefore, it was confirmed that the generated zinc/carboxylate complexes in all samples had the bridge bidentate-type coordination.

The appearance of broad bands at 1595 and 1422 cm^{-1}, however, was different among the samples even when the concentration of fatty acids was equally set among the samples. To confirm the characteristic of aliphatic chain length of fatty acids, the FT-IR spectra of all samples at 144 °C (24.4 min after heating) were investigated in the range of 780–710 cm^{-1}, as shown in Fig. 4. Only IR-ZnO(0.5)-ArH(2.2) showed a clear absorption band at 722 cm^{-1}, which corresponded to the –CH bending in plane rocking of methyl in the long alkyl chain of the fatty acid.[26] Therefore, the interaction between long alkyl chains in IR-ZnO(0.5)-ArH(2.2) may be stronger than that in other samples, which may result in the poor dispersion of ArH in the rubber matrix and low reactivity with ZnO. In fact, the absorption band at 722 cm^{-1} was not detected in other samples. Thus, such phenomena are supposed to occur in fatty acids with longer aliphatic chain length over 20 carbon atoms.

XAFS analysis. To estimate the reactivity between ZnO and different types of fatty acids, the synchrotron zinc K-edge XAFS spectroscopy, which allows to study the local structure around the selected elements in organic and inorganic materials at the atomic and molecular scale, was conducted. Fig. 5 shows normalized and background-subtracted zinc K-edge XAFS spectra of all isoprene rubber compounds for the unvulcanized system in the range of 9620 to 9740 eV during heating from 35 °C to 144 °C and maintaining at 144 °C with those of the reference samples, *i.e.*, IR-ZnO(1) and IR-$ZnSt_2$(4.5) at 35 °C and 144 °C. It was determined that the XAFS spectra of all samples for the unvulcanized system clearly changed during the heating process. These results indicate that the local structure around the Zn atom in each sample changed with an increase in the temperature and time.

In addition, a variation in the intensity and energy at the absorption edge of the zinc K-edge XAFS spectra was different between the samples and depended on the aliphatic chain length of fatty acids. The energy at the absorption edge of the XAFS spectra of all samples for the unvulcanized system and the reference samples at 35 °C ($t = 0$) and 144 °C ($t = 20.1$) are summarized in Table 2. The energies at the absorption edge of the XAFS spectra of IR-ZnO(0.5)-LaH(1.4), IR-ZnO(0.5)-MyH(1.6), and IR-ZnO(0.5)-ArH(2.2) at 35 °C were approximately 9666.0 eV, which corresponded to that of IR-ZnO(1) at 35 °C. These results suggest that the main fraction at 35 °C of IR-ZnO(0.5)-LaH(1.4), IR-ZnO(0.5)-MyH(1.6), and IR-ZnO(0.5)-ArH(2.2) was ZnO. However, IR-ZnO(0.5)-PaH(1.8) and IR-ZnO(0.5)-StH(2.0) showed energies at absorption edge of XAFS spectra of approximately 9662.0 eV, which was similar to that of IR-$ZnSt_2$(4.5) at 35 °C. Thus, the Zn salts, *i.e.*, $Zn(O_2CC_{15}H_{31})_2$ and $Zn(O_2CC_{17}H_{35})_2$, were probably generated in IR-ZnO(0.5)-PaH(1.8) and IR-ZnO(0.5)-StH(2.0), respectively, at 35 °C. These results suggest that PaH (C_{16}) and StH (C_{18}) may have an adequate aliphatic chain length to react with ZnO compared

Table 2 Energy at absorption edge of zinc K-edge XAFS spectra of the isoprene rubber compounds for the unvulcanized systems and the reference samples at 35 °C and 144 °C

	Energy at absorption edge of zinc K-edge XAFS spectrum	
Sample code	35 °C ($t = 0$)	144 °C ($t = 20.1$)
IR-ZnO(0.5)-LaH(1.4)	9666.0	9663.2
IR-ZnO(0.5)-MyH(1.6)	9666.0	9663.1
IR-ZnO(0.5)-PaH(1.8)	9662.1	9662.8
IR-ZnO(0.5)-StH(2.0)	9662.0	9663.0
IR-ZnO(0.5)-ArH(2.2)	9665.9	9664.8
IR-ZnO(1)	9666.0	9665.8
IR-$ZnSt_2$(4.5)	9662.2	9662.8

with that in other types of fatty acids. Thus, the structures of Zn salts of PaH and StH can be readily generated at low temperature (35 °C).

At 144 °C, the energies at the absorption edges of all samples, except for IR-ZnO(0.5)-ArH(2.2), were at approximately 9663.0 eV, which was similar to that of IR-$ZnSt_2$(4.5) at 144 °C. These results indicated that the local structures around the Zn atoms in IR-ZnO(0.5)-LaH(1.4), IR-ZnO(0.5)-MyH(1.6), IR-ZnO(0.5)-PaH(1.8), and IR-ZnO(0.5)-StH(2.0) were similar to that in IR-$ZnSt_2$(4.5) at 144 °C. Thus, the results clearly

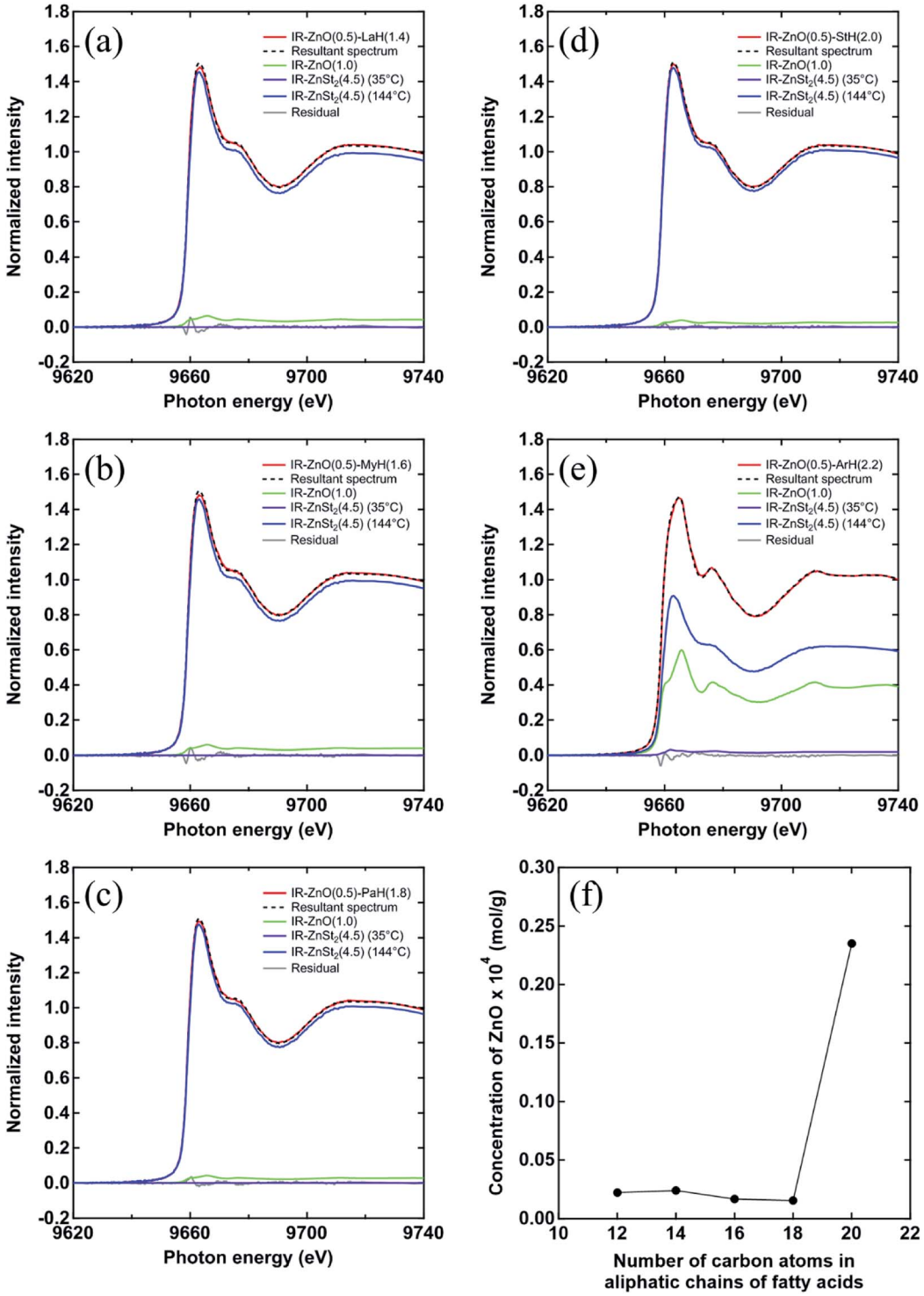

Fig. 6 Fitting results of XAFS spectra at 144 °C (t = 20.1) of (a) IR-ZnO(0.5)-LaH(1.4), (b) IR-ZnO(0.5)-MyH(1.6), (c) IR-ZnO(0.5)-PaH(1.8), (d) IR-ZnO(0.5)-StH(2.0), and (e) IR-ZnO(0.5)-ArH(2.2). (f) The concentrations of unreacted Zn atom in the fitted results of all the samples plotted against number of carbon atom in aliphatic chain of various fatty acids.

indicated that the dinuclear bridging bidentate zinc/carboxylate complexes were formed in those samples, and their chemical structures were possibly similar to that of IR-$ZnSt_2$(4.5) at 144 °C. However, the energy at the absorption edge in the XAFS spectrum of IR-ZnO(0.5)-ArH(2.2) at 144 °C was still observed at approximately 9665 eV, which was in the similar range as that of IR-ZnO(1) at 144 °C. The energy at the absorption edge of the XAFS spectrum of the reference sample, IR-ZnO(1), at 144 °C was insignificantly different from that at 35 °C. It is presumed that the relatively large amount of unreacted ZnO remained in IR-ZnO(0.5)-ArH(2.2) even at high temperature.

In order to evaluate the fractions of unreacted ZnO, the Zn salt of fatty acid and the dinuclear bridging bidentate zinc/carboxylate complex, the linear combination fitting of XAFS spectra at 144 °C of all samples for the unvulcanized system were conducted using IR-ZnO(1) at 144 °C, IR-$ZnSt_2$(4.5) at 35 °C and IR-$ZnSt_2$(4.5) at 144 °C, as the reference model compounds, respectively. The fitting results of their XAFS spectra are shown in Fig. 6(a)–(e). All samples showed the sufficiently well-fitted spectra with small residuals. At 144 °C, the dinuclear bridging bidentate zinc/carboxylate complexes were predominantly formed in IR-ZnO(0.5)-LaH(1.4), IR-ZnO(0.5)-MyH(1.6), IR-ZnO(0.5)-PaH(1.8), and IR-ZnO(0.5)-StH(2.0). The small fraction of unreacted ZnO and the disappearance of Zn salts of fatty acids were also detected in those samples. The fractions of the dinuclear bridging bidentate zinc/carboxylate complexes of IR-ZnO(0.5)-PaH(1.8) and IR-ZnO(0.5)-StH(2.0) were slightly higher, whereas their fractions of unreacted ZnO were smaller compared with those of IR-ZnO(0.5)-LaH(1.4) and IR-ZnO(0.5)-MyH(1.6) at 144 °C. This difference was quantitatively confirmed that not only the Zn salts of PaH and StH [*i.e.*, $Zn(O_2CC_{15}H_{31})_2$ and $Zn(O_2CC_{17}H_{35})_2$, respectively] but also their dinuclear bridging bidentate zinc/carboxylate complexes were readily generated in IR-ZnO(0.5)-PaH(1.8) and IR-ZnO(0.5)-StH(2.0) at 144 °C because of the adequate aliphatic chain lengths of PaH (C_{16}) and StH (C_{18}).

Although, the main fraction in IR-ZnO(0.5)-ArH(2.2) was the dinuclear bridging bidentate zinc/carboxylate complex, the fraction of unreacted ZnO was clearly detected and was much higher than that of other samples. The concentration of unreacted Zn atom in the fitted results of all samples was calculated according to eqn (3) and plotted against the number of carbon atom in aliphatic chain of various fatty acids, as shown in Fig. 6(f). It was confirmed that ZnO was not completely consumed in IR-ZnO(0.5)-ArH(2.2) and approximately 0.24×10^{-4} mol g^{-1} of Zn atoms remained even when the temperature reached to 144 °C. These results support the presence of energy at the absorption edge of the XAFS spectrum at approximately 9665 eV for IR-ZnO(0.5)-ArH(2.2) at 144 °C (Fig. 5(e) and Table 2). The relatively higher amount of unreacted ZnO in IR-ZnO(0.5)-ArH(2.2) than those in other samples is ascribable to the stronger interaction between the longer alkyl chain of ArH. Thus, the self-aggregation of ArH occurred, and the reactivity with ZnO became low. These results correspond well with the presence of the FT-IR absorption band at 722 cm^{-1} (–CH in plane rocking of methyl in the long alkyl chain of fatty acid).

Here, we noticed the contradiction that the bands of carboxylic C=O antisymmetric stretching in a monomer and a dimer of ArH were not detected at approximately 1760–1715 cm^{-1} in IR-ZnO(0.5)-ArH(2.2), even though ZnO was remained. Probably, it is ascribable to ZnO clusters with bound carboxylate surface-functionalization by ArH, which is formed at 144 °C. In such a specific carboxylate group on ZnO, for example, the broadened carboxylate antisymmetric and symmetric vibrational modes were reported to shift to the low wavenumber for stearic acid.[25,27] The detail will be reported in a near future.

Furthermore, the XAFS spectra of all samples, including IR-ZnO(0.5)-ArH(2.2), after the subtraction of remaining ZnO are shown in Fig. 7. All samples at 144 °C showed the same energies at the absorption edge of XAFS spectra as that of IR-$ZnSt_2$(4.5) at 144 °C (a reference sample), which was approximately 9663 eV. This observation suggests that each sample can form a tetrahedral coordination structure of dinuclear-type bridging bidentate of zinc/carboxylate complex at high temperature, similarly with our previous results observed in isoprene rubber mixed with $ZnSt_2$ or ZnO/StH, as reported.[13,14] Therefore, the XAFS and FT-IR results suggested that the aliphatic chain length of fatty acids does not affect the generation of the dinuclear bridging bidentate zinc/carboxylate complex intermediate in the rubber matrix at high temperature, however, it influences the reactivity of the fatty acid with ZnO.

Curing behavior by active intermediates generated from different fatty acids

In the previous section, the dinuclear bridging bidentate zinc/carboxylate complexes were determined to be generated from ZnO and fatty acids. These intermediates must accelerate the sulfur cross-linking reaction of rubber. Here, the effect of these dinuclear bridging bidentate zinc/carboxylate complexes

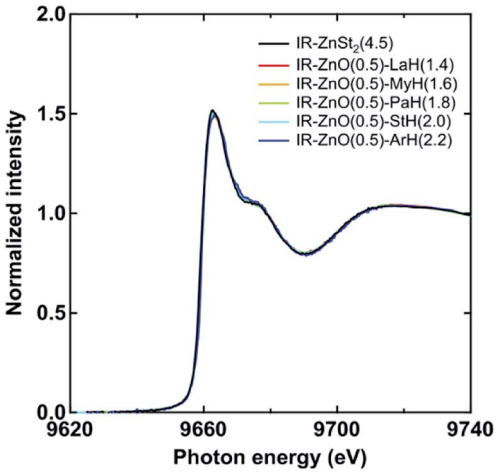

Fig. 7 Zinc K-edge XAFS spectra of IR-ZnO(0.5)-LaH(1.4), IR-ZnO(0.5)-MyH(1.6), IR-ZnO(0.5)-PaH(1.8), IR-ZnO(0.5)-StH(2.0), IR-ZnO(0.5)-ArH(2.2) and IR-$ZnSt_2$(4.5) at 144 °C in the range of 9620–9740 eV. Those spectra were obtained by normalizing and subtracting the spectra of unreacted ZnO based on the fitting results in Fig. 6.

containing different fatty acid ligands on the vulcanization reactions of vulcanized rubbers was investigated. The viscoelasticity of rubber compounds obtained from rheological measurement was used to monitor the vulcanization reaction. Fig. 8 shows a change in G' and G'' of all vulcanized samples during heating to 144 °C *vs.* the heating time. G' and G'' are related to the elastic and viscous responses of the viscoelastic rubber material after applying shear stress. In addition, the cross point of G' and G'' is generally known as the gelation point,[28,29] where the three-dimensional network structure is formed through the whole polymer chains by cross-linking. As shown in Fig. 8, the values of G'' (approximately 3 min after heating) of all samples were higher than those of G'. This may be due to the softening of rubber by heating and the plasticizing by fatty acids. Interestingly, it was determined that the gelation time (Table 3) tended to increase in the sample with a longer aliphatic chain length of fatty acid, as shown in Fig. 8(f). Specifically, the gelation time of IR-ZnO(0.5)-ArH(2.2)-CBS(1)-S_8(1.5) was much longer than that of other samples by approximately 2–3 min. These results suggest that the induction

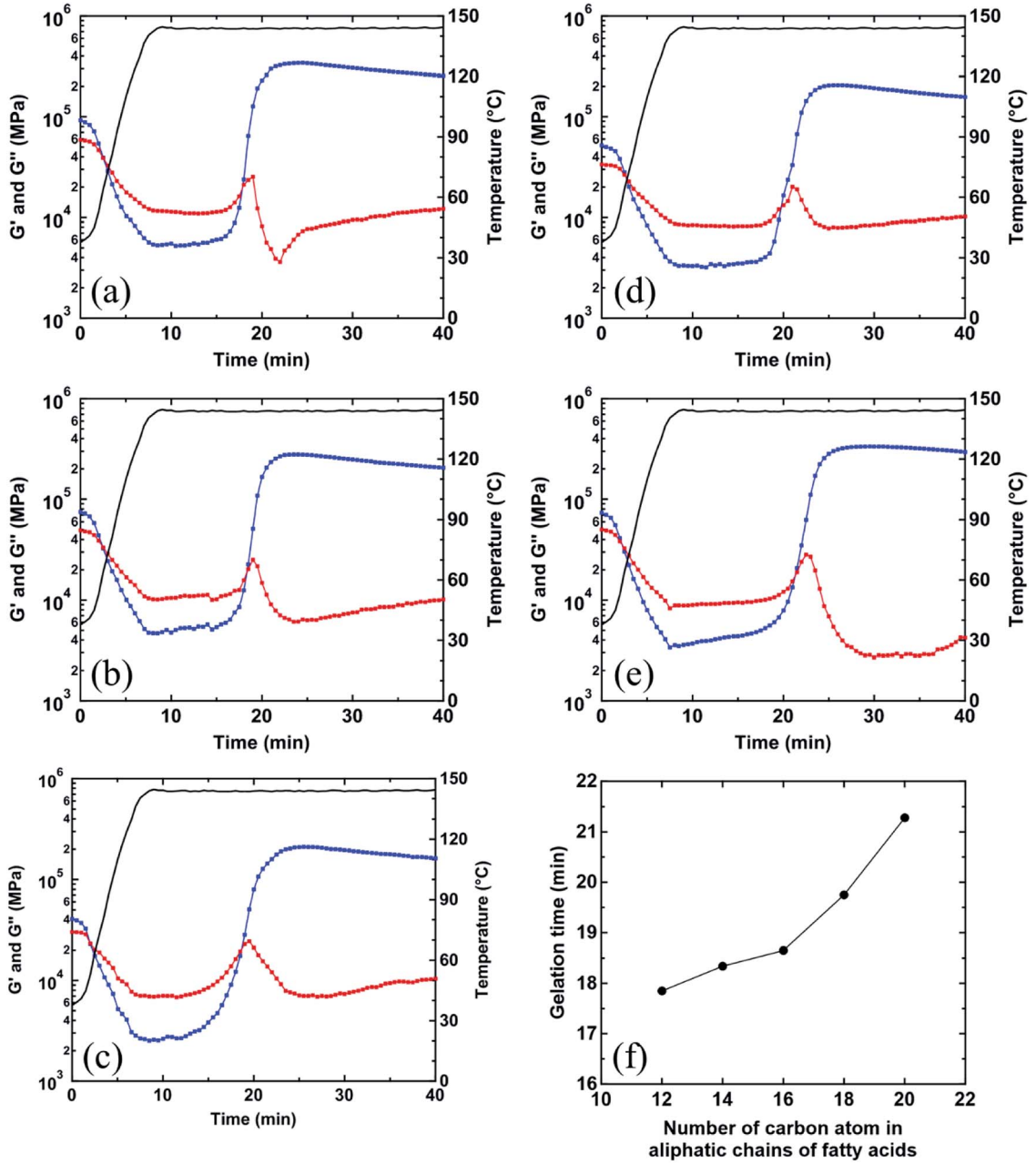

Fig. 8 Variations of shear storage moduli (G') (blue trace) and shear loss moduli (G'') (red trace) of the heating process from 35 to 144 °C and the constant temperature condition at 144 °C for (a) IR-ZnO(0.5)-LaH(1.4)-CBS(1)-S_8(1.5), (b) IR-ZnO(0.5)-MyH(1.6)-CBS(1)-S_8(1.5), (c) IR-ZnO(0.5)-PaH(1.8)-CBS(1)-S_8(1.5), (d) IR-ZnO(0.5)-StH(2.0)-CBS(1)-S_8(1.5), and (e) IR-ZnO(0.5)-ArH(2.2)-CBS(1)-S_8(1.5). (f) The gelation time plotted against the number of carbon atom in aliphatic chains of various fatty acids.

Table 3 Calculated t_0, t_{dis}, t_{max}, $(M_H - M_L)$ and K of the samples in the vulcanized system

Sample code	t_0 (min)	t_{dis} (min)	t_{max}[a] (min)	$(M_H - M_L) \times 10^3$ (N m)	K (min^{-1})
IR-ZnO(0.5)-LaH(1.4)-CBS(1)-S_8(1.5)	15.5	4.5	24.5	3.2	1.02
IR-ZnO(0.5)-MyH(1.6)-CBS(1)-S_8(1.5)	15.5	4.0	23.5	2.6	0.97
IR-ZnO(0.5)-PaH(1.8)-CBS(1)-S_8(1.5)	15.5	6.5	25.5	3.0	1.00
IR-ZnO(0.5)-StH(2.0)-CBS(1)-S_8(1.5)	16.5	5.5	26.5	2.9	0.96
IR-ZnO(0.5)-ArH(2.0)-CBS(1)-S_8(1.5)	16.5	7.0	29.5	4.8	0.88

[a] Time at M_H.

period before sulfur cross-linking may be affected by the generated dinuclear bridging bidentate zinc/carboxylate complex intermediates, depending on the kind of fatty acids. The longer fatty acid ligands in the bridging bidentate zinc/carboxylate complexes possibly make it more difficult to further react with the vulcanizing agents, *i.e.*, CBS and sulfur.

After gelation points, G'', which typically corresponds to the dissipation of strain energy, slightly increased in all samples before suddenly decreasing. These phenomena may be related to the diversification to infinite molecular weight by sulfur cross-linking after the gel point. However, G' continuously increased to a certain extent and was much higher than G'' at the same heating time. These data suggest that the formation of three-dimensional cross-linking network provides a more elastic response than viscous response in the vulcanized samples. At the long heating time after the gelation point, the values of G′ slightly decreased, whereas those of G'' tended to increase, which indicate the reversion of sulfur cross-linking at this stage.

In order to clearly confirm the influence of the bridging bidentate zinc/carboxylate complexes containing different fatty acid ligands on the kinetics of the vulcanization reaction of rubbers, the curing behavior during heating to 144 °C of the vulcanized samples was evaluated by rheological analysis as shown in Fig. 9(a). According to eqn (2), the plot of $\ln(M_H - M_t)$ *vs.* $(t - t_0)$ for each vulcanized sample is displayed, and the data that follow the first order of the reaction ($n = 1$) were extracted, as shown in Fig. 9(b). The parameters K, including $(M_H - M_L)$, t_0, and t_{dis}, for each vulcanized sample are summarized in Table 3. Here, t_{dis} is the time difference between the initial heating time (t_0) and time when the first-order reaction starts.[18] The values of t_{dis} (Table 3), which are related to the time at which the accelerators or intermediates react to completion,[18] were different among the vulcanized samples. The vulcanizates prepared by the zinc/carboxylate complexes with a longer aliphatic chains showed later t_{dis}. This tendency was similar to that of gelation time (Fig. 8(f)) of the vulcanized samples, as mentioned above. The K values of all vulcanizates, except for IR-ZnO(0.5)-ArH(2.2)-CBS(1)-S_8(1.5), were approximately 1.0 min^{-1}, whereas that of IR-ZnO(0.5)-ArH(2.2)-CBS(1)-S_8(1.5) was 0.88 min^{-1}, which was lower than those of other samples.

These results can be explained from the viewpoint of the two-phase inhomogeneous network morphology of sulfur cross-linked isoprene rubber in the CBS-accelerated curing system with ZnO and StH, where the network domains of high network-chain density are embedded in the mesh network.[11,12,15] The mesh network is formed by the dinuclear bridging bidentate zinc/stearate complex. Thus, the concentration of zinc stearate is a key factor for controlling the mesh size in the matrix. The network domains, on the other hand, are formed around ZnO clusters by absorbing sulfur and CBS and followed by sulfur cross-linking. The formation of mesh network is determined to occur slightly earlier than that of the network domains using a combination of *in situ* zinc K-edge XAFS and DSC measurements.[12] This is probably due to the acceleration of sulfur cross-linking of the mesh network by the dinuclear bridging bidentate zinc/stearate complex intermediate.[12–14] In the previous section, ArH showed a relatively lower reactivity with ZnO in the rubber matrix than those of the other types of fatty acids. In addition,

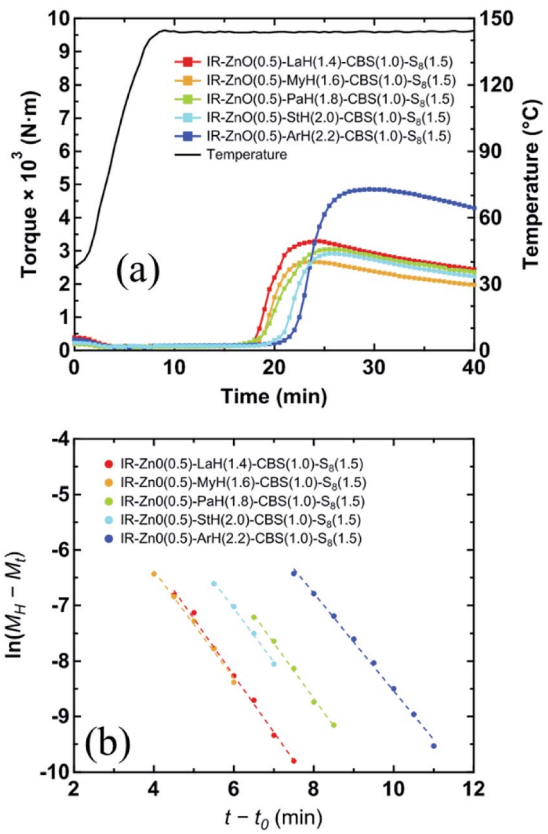

Fig. 9 (a) Cure curves of the samples in the vulcanized system. (b) Variation of $\ln(M_H - M_t)$ plotted against $(t - t_0)$ of the samples.

using a linear combination fitting of the XAFS spectrum, it was determined that approximately 0.24×10^{-4} mol g^{-1} of unreacted ZnO still remained in IR-ZnO(0.5)-ArH(2.2)-CBS(1)-S_8(1.5) at 144 °C. Therefore, the slower starting of sulfur cross-linking reaction around ZnO particles may significantly influence the overall cross-linking reaction rate, compared with that of the mesh network formation *via* the dinuclear bridging bidentate zinc/carboxylates complexes. Thus, the dinuclear bridging bidentate zinc/carboxylate complex intermediate was determined to affect the vulcanization reaction in both induction and curing periods, depending on the aliphatic chain length of the fatty acids.

Fig. 10(a) shows the DSC curves at 144 °C of all vulcanized samples. An exothermic peak was observed in the DSC curves of all samples, which was an indication of the exothermic reaction of vulcanization of rubber. The time at which peaks started to appear and reached to maximum were defined as t_{init} and t_{max}, respectively. The values of t_{init} and t_{max} of all vulcanized samples were plotted *vs.* the number of carbon atoms in the aliphatic chain of various fatty acids, as shown in Fig. 10(b). The values of t_{init} and t_{max} changed in the ranges of 15.0–19.7 and 21.5–23.6 min, respectively. The longer t_{init} and t_{max} were determined in the vulcanized sample with an increase in the aliphatic chain length of the fatty acid. This tendency is also similar to that of the gelation time, cure rate constant, and t_{dis} measured by rheological measurements. Therefore, it is clear that the dinuclear bridging bidentate zinc/carboxylate complexes containing different fatty acid ligands in the samples affected the vulcanization reactions. Thus, the longer aliphatic chain length in the intermediate complex resulted in the slower vulcanization reaction.

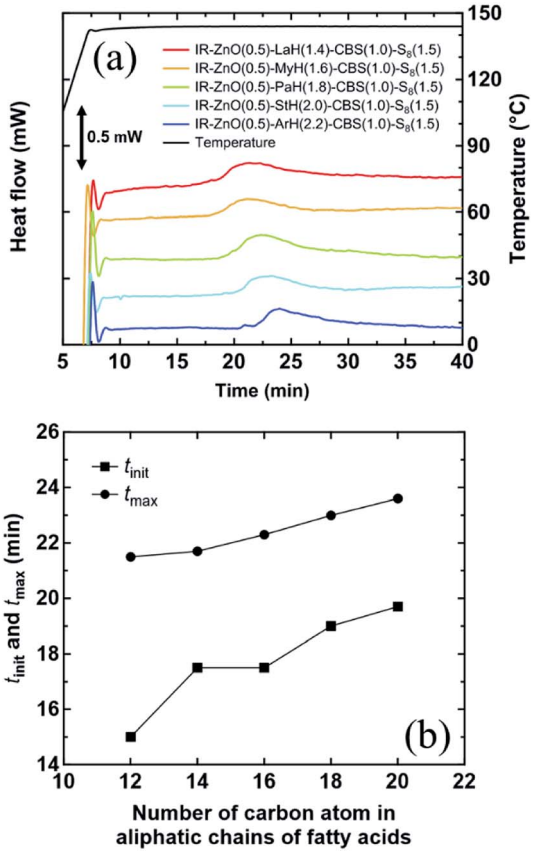

Fig. 10 (a) DSC curves of the heating process from 35 to 144 °C and the constant temperature condition at 144 °C for IR-ZnO(0.5)-LaH(1.4)-CBS(1)-S_8(1.5), IR-ZnO(0.5)-MyH(1.6)-CBS(1)-S_8(1.5), IR-ZnO(0.5)-PaH(1.8)-CBS(1)-S_8(1.5), IR-ZnO(0.5)-StH(2.0)-CBS(1)-S_8(1.5), and IR-ZnO(0.5)-ArH(2.2)-CBS(1)-S_8(1.5). (b) The plots of t_{init} and t_{max} against the number of carbon atom in the aliphatic chains of various fatty acids.

Bio-activators for the vulcanization reaction of NR

NR, which is currently widely used, is obtained from the milky fluid tapped from the Para rubber tree, *Hevea brasiliensis*. NR latex consists of rubber hydrocarbon of approximately 30–45 wt% and non-rubber components of approximately 3–5 wt%. The other constituent is water. Among the non-rubber components, NR was reported to contain various fatty acids as a mixture including saturated fatty acids (*e.g.*, decanoic acid, myristic acid, palmitic acid, and stearic acid) and unsaturated fatty acids (*e.g.*, palmitoleic acid, oleic acid, linoleic acid, and linoleinic acid). These fatty acids are also expected to partially link to the rubber molecule as phospholipids.[30] The mixed fatty acids, which are inherently present in NR, have been proposed to be a bio-activator for vulcanization in NR. However, the actual role of these bio-activators on the vulcanization reaction of NR remains unclear. This study may give a hint to answer for this question.

Fig. 11 shows the *in situ* FT-IR spectra of NR-ZnO(0.5) from 35 to 144 °C. Without StH, two broad bands at 1530 and 1550 cm^{-1} appeared, which were in the range of the COO^- antisymmetric stretching for $ZnSt_2$, as detected in the FT-IR spectra of IR-ZnO(0.5)-StH(2) at 35 °C in our previous study.[13,14] With further heating to 144 °C, the intensities of absorption band at both 1530 and 1550 cm^{-1} decreased and that of one broad band at 1595 cm^{-1} increased. These changes in the FT-IR spectra of all samples upon heating to 144 °C were

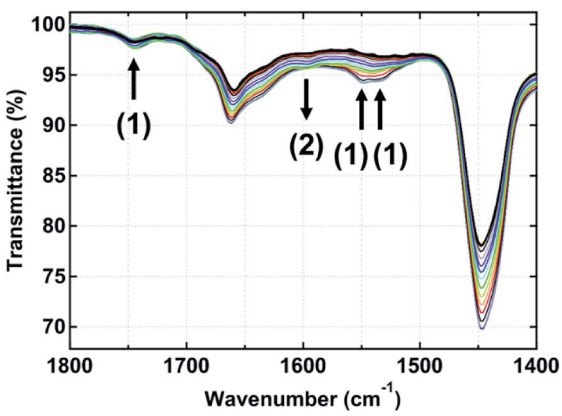

Fig. 11 FT-IR spectra of NR-ZnO(0.5) of the heating process from 35 to 144 °C and the constant temperature condition at 144 °C in the range of 1800–1400 cm^{-1}. Numbers and black arrows indicate the order and the direction of band shifts during heating, respectively.

similar to those of IR-$ZnSt_2$(4.5). These results indicate the possible formation of active intermediate dinuclear bridging bidentate zinc/carboxylate complexes, as observed in the model isoprene rubber samples, as mentioned in the previous section. However, all characteristic absorption bands for the Zn salt of fatty acids and active intermediates in NR-ZnO(0.5) were broader, and their intensities were weaker than those of model isoprene rubber samples. This occurs because of the mixture of fatty acids and a smaller amount of the mixed fatty acids present in the NR sample. Thus, StH is usually added to the rubber compounding recipe of NR for the suitable NR compounding conditions. Even though there are still unidentified absorption bands in the FT-IR spectra of NR-ZnO(0.5) that are not observed in the spectra of model isoprene rubber samples, to our knowledge, these preliminary *in situ* FT-IR results of NR-ZnO(0.5) from 35 to 144 °C and the constant temperature condition at 144 °C confirm for the first time the reactivity of bio-activators with ZnO in NR during heating. To better understand the mechanism of the vulcanization reaction of NR, the combination of other experimental techniques should be considered.

Conclusion

The model rubber compounds of isoprene rubber containing ZnO and various types of saturated fatty acids were prepared for the first time to investigate the influence of organic activator on the vulcanization reaction in rubber. Using the *in situ* measurements of zinc K-edge XAFS spectroscopy and *in situ* time-resolved FT-IR spectroscopy, the generation of zinc/carboxylate complex intermediate in isoprene rubbers containing ZnO and fatty acid at high temperature was confirmed. The fundamental skeletons of those intermediates were confirmed to have the dinuclear bridging bidentate-type coordination. However, the long aliphatic chain length of fatty acids (*i.e.*, 20 carbon atoms) resulted in the low reactivity with ZnO because of the high melting temperature. In addition, the dinuclear bridging bidentate zinc/carboxylate complex intermediates with different fatty acid ligands were determined to affect the cross-linking reaction.

The vulcanized sample with a long aliphatic chain length appeared to prolong the induction period and curing time. Nevertheless, the curing rates of rubber vulcanizates were not considerably different, except for the vulcanized sample with a fatty acid having the aliphatic chain length of 20 carbon atoms. This observation is attributable to the higher steric hindrance in the structure of dinuclear bridging bidentate zinc/carboxylate complex intermediate with a long aliphatic chain length of the fatty acid, which makes it more difficult to further react with the curing agents during the vulcanization reaction.

Although it is well-known that fatty acids are organic activators that are widely used in the rubber industry, this is the first report on role of fatty acids during the vulcanization reaction of rubber. This basic and important result is useful to better understand the complicated vulcanization reaction of rubber, especially that of NR. Because NR contains various acids, the new observation in this study will be valuable for the development of NR science for the 21st century. Eventually, the obtained results will become a fundamental knowledge for making the controllable cross-linking network structure in rubber for the manufacturing of well-designed high-performance rubber products.

Conflicts of interest

There are no conflicts to declare.

Acknowledgements

This work was supported by JST ALCA program (grant number: JPMJAL1501). The XAFS experiments were performed at the BL-14B2 in the SPring-8 with the approval of the Japan Synchrotron Radiation Research Institute (JASRI) (proposal no. 2009A1929, 2009B2044, 2010A1778, 2010B1928, 2012A1419, 2012B1891, 2013A1828, 2013B1840, 2014A1574, 2017A1611, 2017B1631, 2017B1922). The authors also thank to Mr T. Ohashi and Dr P. Taranamai for their advices.

Notes and references

1 L. Bateman, C. G. Moore, M. Porter and B. Saville, in *The Chemistry and Physics of Rubber-like Substances*, ed. L. Bateman, MacLaren Sons Ltd, London, 1963, ch. 19.
2 M. M. Coleman, J. R. Shelton and J. L. Koenig, *Ind. Eng. Chem. Prod. Res. Dev.*, 1974, **13**, 154–166.
3 C. D. Trivette, E. Morita and O. W. Maender, *Rubber Chem. Technol.*, 1977, **50**, 570–600.
4 E. Morita, *Rubber Chem. Technol.*, 1980, **53**, 393–436.
5 A. V. Chapman and M. Porter, in *Natural Rubber Science and Technology*, ed. A. D. Roberts, Oxford University Press, Oxford, 1988, ch. 12, pp. 511–620.
6 A. Y. Coran, in *The Science and Technology of Rubber*, ed. J. E. Mark, B. Erman and F. R. Eirich, Academic Press, San Diego, 2nd edn, 1994, ch. 7, pp. 339–385.
7 A. Y. Coran, *J. Appl. Polym. Sci.*, 2003, **87**, 24–30.
8 P. Ghosh, S. Katare, P. Patkar, J. M. Caruthers, V. Venkatasubramanian and K. A. Walker, *Rubber Chem. Technol.*, 2003, **76**, 592–693.
9 G. Heideman, R. N. Datta, J. W. M. Noordermeer and B. van Baarle, *Rubber Chem. Technol.*, 2004, **77**, 512–541.
10 Y. Ikeda, A. Kato, S. Kohjiya and Y. Nakajima, *Rubber Science: A Modern Approach*, Springer, Singapore, 2017.
11 Y. Ikeda, N. Higashitani, K. Hijikata, Y. Kokubo, Y. Morita, M. Shibayama, N. Osaka, T. Suzuki, H. Endo and S. Kohjiya, *Macromolecules*, 2009, **42**, 2741–2748.
12 Y. Yasuda, S. Minoda, T. Ohashi, H. Yokohama and Y. Ikeda, *Macromol. Chem. Phys.*, 2014, **215**, 971–977.
13 Y. Ikeda, Y. Yasuda, T. Ohashi, H. Yokohama, S. Minoda, H. Kobayashi and T. Honma, *Macromolecules*, 2015, **48**, 462–475.
14 Y. Ikeda, Y. Sakaki, Y. Yasuda, P. Junkong, T. Ohashi, K. Miyaji and H. Kobayashi, *Organometallics*, 2019, **38**, 2363–2380.

15 T. Ohashi, T. Sato, T. Nakajima, P. Junkong and Y. Ikeda, *RSC Adv.*, 2018, **8**, 32930–32941.
16 Y. Sakaki, R. Usami, A. Tohsan, P. Junkong and Y. Ikeda, *RSC Adv.*, 2018, **8**, 10727–10734.
17 A. Tohsan, Y. Yasuda, R. Usami, T. Ohashi, Y. Sakaki, P. Junkong and Y. Ikeda, *Kautsch. Gummi, Kunstst.*, 2018, **6**, 111–115.
18 Y. W. Ping, L. Q. Hong, P. Y. He and C. Jin, *J. Appl. Polym. Sci.*, 2003, **88**, 680–684.
19 T. Honma, H. Oji, S. Hirayama, Y. Taniguchi, H. Ofuchi and M. Takagaki, *AIP Conf. Proc.*, 2010, **1234**, 13–16.
20 SPring-8: Industrial Application Division, http://support.spring8.or.jp/xafs.html, accessed March 20, 2019.
21 B. Ravel and M. Newville, *J. Synchrotron Radiat.*, 2005, **12**, 537–541.
22 A. L. Ankudinov, B. Ravel, J. J. Rehr and S. D. Conradson, *Phys. Rev. B*, 1998, **58**, 7565–7576.
23 J. J. Rehr and A. L. Ankudinov, *Coord. Chem. Rev.*, 2005, **249**, 131–140.
24 G. B. Deacon, *Coord. Chem. Rev.*, 1980, **33**, 227–250.
25 K. Nakamoto, *Infrared and Raman Spectra of Inorganic and Coordination Compounds: Part B: Applications in Coordination, Organometallic, and Bioinorganic Chemistry*, Wiley, New York, 5th edn, 1997.
26 M. Hesse, H. Meier and B. Zeeh, *Spectroscopic Methods in Organic Chemistry*, Thieme Medical Publishers, Inc., NY, 2nd edn, 2007.
27 K. L. Orchard, M. S. P. Shaffer and C. K. Williams, *Chem. Mater.*, 2012, **24**, 2443–2448.
28 P. J. Flory, *J. Am. Chem. Soc.*, 1941, **63**, 3083–3090.
29 P. J. Flory, *J. Am. Chem. Soc.*, 1941, **63**, 3096–3100.
30 C. C. Ho, A. Subramaniam and W. M. Young, *Proceedings of the International Rubber Conference*, Rubber Research Institute of Malaysia, Kuala Lumpur, 1975, vol. 2, pp. 441–456.